# Gas-Phase Ion−Molecule Reactions in $C_3F_6$

**Kenzo Hiraoka,* Kiyotoshi Takao, Tomoyuki Iino, Fumiyuki Nakagawa, Hiroko Suyama, and Takayuki Mizuno**

*Clean Energy Research Center, Yamanashi University, Takeda, Kofu 400-8511, Japan*

**Shinichi Yamabe***

*Department of Chemistry, Nara University of Education, Takabatake-cho, Nara 630-8528, Japan*

*Received: April 30, 2001; In Final Form: August 9, 2001*

Gas-phase ion−molecule reactions in hexafluoropropene ($C_3F_6$) were studied with a pulsed electron beam mass spectrometer. In the reactions of $C_3F_6^+$ and $C_2F_4^+$ ions with $C_3F_6$ to form $C_3F_6^+(C_3F_6)_n$ and $C_2F_4^+(C_3F_6)_n$, respectively, the equilibria could not be observed but the cluster ions $C_3F_6^+(C_3F_6)_n$ and $C_2F_4^+(C_3F_6)_n$ were found to grow very slowly at the expense of the smaller cluster ions $C_3F_6^+(C_3F_6)_{n-1}$ and $C_2F_4^+(C_3F_6)_{n-1}$, respectively. The decay rates of $C_3F_6^+(C_3F_6)_{n-1}$ and $C_2F_4^+(C_3F_6)_{n-1}$ to form $C_3F_6^+(C_3F_6)_n$ and $C_2F_4^+(C_3F_6)_n$, respectively, become faster at lower temperature. This is due to the existence of an entropy barrier for the formation of cluster ions. The $C_3F_5^+$ ion was found to form cluster ions readily with $C_3F_6$ solvent molecules. Thermochemical stabilities for $C_3F_5^+(C_3F_6)_n$ with $n = 1$ and 2 could be determined. The proton affinity (PA) of $C_3F_6$ was found to be smaller but close to that of $C_2H_4$ (162.6 ± 1.5 kcal/mol). The G2MP2-calculated PA is 157.26 kcal/mol. Lone-pair orbitals of the $CF_3$ substituent are electronic-charge donor sites to $C_2F_4^+$ and $C_3F_5^+$. The polymerization reactions of $C_3F_6$ initiated by $F^-$, $C_3F_5^-$, and $C_3F_6^-$ were observed. Those reactions became faster with a decrease of temperature. The high reactivity of $C_3F_6$ in the negative-mode ion/molecule reactions is ascribed to the perfluoro effect. The halide ions $Cl^-$, $Br^-$, and $I^-$ were found to form cluster ions with $C_3F_6$. Thermochemical stabilities for $X^-(C_3F_6)_n$ ($X^- = Cl^-$, $Br^-$, and $I^-$) have been determined. A slight charge transfer in the complex $Cl^-\rightarrow C_3F_6$ results in the fairly strong bond energy (12.6 kcal/mol) for the cluster.

## 1. Introduction

Gas-phase ion−molecule reactions including saturated and unsaturated hydrocarbons have been the subject of many investigators.[1−8] In particular, the polymerization of $C_2H_4$ induced by the primary $C_2H_4^+$ ion has been a topic of continuous and considerable interest for several decades.[1−3,6,8] Kebarle and Haynes[2] showed that the reaction of $C_2H_4^+$ with $C_2H_4$ molecules did not form cluster ions but rather formed covalently bonded molecular ions, $C_2H_4^+\cdot C_2H_4$. The $C_2H_4^+$ ion readily underwent cationic polymerization of up to $n = 4$ monomers via sequential exothermic reactions. But the polymer growth was terminated at this *n*. Castleman et al. examined the intracluster polymerization reactions of $C_2H_4$ cluster ions.[7] These ions were prepared by the supersonic expansion of a premixed sample gas of $C_2H_4$ and Ar. They concluded that after photoionization, intracluster polymerization initiated by a radical cation $C_2H_4^+$ takes place in the cluster ions. However, due to steric hindrance, polymerization proceeds only up to pentamization and the nature of bonding becomes electrostatic for larger ions. Thus, the formation of the core pentamer cation with surrounding $C_2H_4$ ligands, $(C_2H_4)_5^+\cdots(C_2H_4)_{n-5}$ was proposed. In our previous paper,[8] the reactions of $C_2H_3^+$, $C_2H_4^+$, and also $C_2H_5^+$ with $C_2H_4$ as functions of the ion source temperature and the $C_2H_4$ pressure were investigated. The larger polymerized ions were formed at lower temperature. For $C_2H_4^+\cdot nC_2H_4$, the polymerization reaction with $n > 5$ was found to take place with a decrease of ion source temperature.

Despite the wealth of investigations on the positive ion/molecule reactions in alkenes, studies on the reactions of negative ions with alkenes are scarce. In our recent paper,[9] the reactivity of halide ions toward $C_2H_4$ and $C_3H_6$ has been investigated. It was found that the four halide ions investigated are bound with $C_2H_4$ and $C_3H_6$ merely by weak electrostatic interactions and they do not initiate the polymerization reaction with those olefins.

When the H atoms of the olefins are substituted by the F atoms, the $\pi$ nature of the C=C double bond is reduced and thus the $\pi$ (HOMO) and $\pi^*$ (LUMO) orbitals will be stabilized (perfluoro effect[10]). This may result in the drastic difference in the reactivities between olefins and perfluoro-olefins. Despite the fact that the perfluoro-olefins have been widely used as useful etchants for the semiconductor fabrication, investigations on the ion/molecule reactions in these reagent gases were relatively scarce. Morris et al. investigated the gas-phase reactions of $CF^+$, $CF_2^+$, $CF_3^+$, $C_2F_3^+$, $C_2F_4^+$, $C_3F_5^+$, and $C_3F_7^+$ with $C_2F_4$ using a variable temperature selected-ion flow tube instrument at 300 and 496 K.[11] They found a variety of types of reactions of those ions with $C_2F_4$, including charge transfer, fluoride transfer, and association. The reaction of $C_2F_4^+$ with $C_2F_4$ is slow, has strong negative temperature dependence, and

* Authors to whom correspondence should be addressed.

10.1021/jp0116306 CCC: $22.00 
Published on Web 01/04/2002

produces $C_3F_5^+$ which is itself unreactive with $C_2F_4$. Hunter et al. studied the electron attachment properties of $C_3F_6$ in $N_2$ and Ar buffer gases.[12] They found that the attachment rate constants have an anomalous dependence on the $C_3F_6$ partial pressure. In an attempt to identify the products of electron attachment, they resorted to a quadrupole mass spectrometer with a corona-discharge electron source operating in a 4% $C_3F_6$ mixture in Ar, at a pressure of ~200 Torr. The resulting major anion products observed were $(C_3F_6)_2^-$, $C_3F_5^-(C_3F_6)$, and $F^-(C_3F_6)_n$ with $n = 1-3$. To explain their findings, they proposed that an electron attaches associatively to a $C_3F_6$ molecule forming a comparatively long-lived intermediate parent negative ion $C_3F_6^-$*. This combines then with a neutral $C_3F_6$ molecule to form a short-lived dimer anion which can be stabilized by the buffer gas M, namely

$$e^- + C_3F_6 \rightarrow C_3F_6^-* \quad (1)$$

$$C_3F_6^-* + C_3F_6 \rightarrow (C_3F_6)_2^-* \quad (2)$$

$$(C_3F_6)_2^-* + M \rightarrow (C_3F_6)_2^- + M \quad (3)$$

Jarvis et al.[13] used an ion-mobility mass spectrometer for the investigation of electron attachment to $C_3F_6$. They confirmed that the electron attachment reaction of $C_3F_6$ is second order with respect to the $C_3F_6$ pressure as Hunter et al. suggested.[12] They found that the reaction product $C_3F_5^-(C_3F_6)$ is not a cluster ion but a covalently bonded molecular ion.

In the present work, the positive- and negative-mode ion/molecule reactions in $C_3F_6$ have been investigated in detail. Contrary to the inertness of $C_2H_4$ and $C_3H_6$ molecules toward halide ions,[9] the $F^-$ ion was found to initiate the polymerization reaction with $C_3F_6$ molecules indicating that the perfluoro effect greatly enhances the reactivity of $C_3F_6$ in the negative mode ion/molecule reactions. The rates of polymerization reactions increased with decrease of temperature (i.e., existence of an entropy barrier but no energy barrier).

## 2. Experimental and Theoretical Methods

The experiments were carried out with a pulsed electron beam high-pressure mass spectrometer.[14,15] Briefly, about 3 Torr of the major gas, $N_2$ or $CH_4$, was purified by passing it through a dry ice acetone-cooled 5 Å molecular sieve trap. The reagent gas, $C_3F_6$, and the halide-ion ($X^-$) forming reagent gases, $NF_3$ for $F^-$, $CCl_4$ for $Cl^-$, $CH_2Br_2$ for $Br^-$, and $CH_3I$ for $I^-$, were introduced into the major gas through flow-controlling stainless steel capillaries. To obtain reliable van't Hoff plots, the equilibrium constants were measured down to the condensation points of the reagent gas $C_3F_6$ or the $X^-$-forming reagent gases.

Geometries of $C_2H_4^+(C_2H_4)_n$ ($n = 1-5$), $C_2F_4^+(C_3F_6)_n$, $C_3F_5^+(C_3F_6)_n$, $X^-(C_3F_6)_n$ ($n = 1$ and 2), and protonated $C_3F_6$ were determined with density-functional-theory (B3LYP).[16] The B3LYP/6-31G* method was used for cationic systems, and the B3LYP/6-31+G* one was used for anionic systems, $X^-(C_3F_6)_n$ (X = F and Cl), respectively. The plus sign in 6-31+G* denotes diffuse sp basis functions which are indispensable to describe energies of the anionic systems properly.[17] The G2MP2 method[18] was also used to evaluate the proton affinity (PA) of $C_3F_6$. The method is known to reproduce experimental PA values accurately.[19] All the calculations were performed by the use of GAUSSIAN 98[20] which was installed at Compaq ES 40 computer (Nara University of Education).

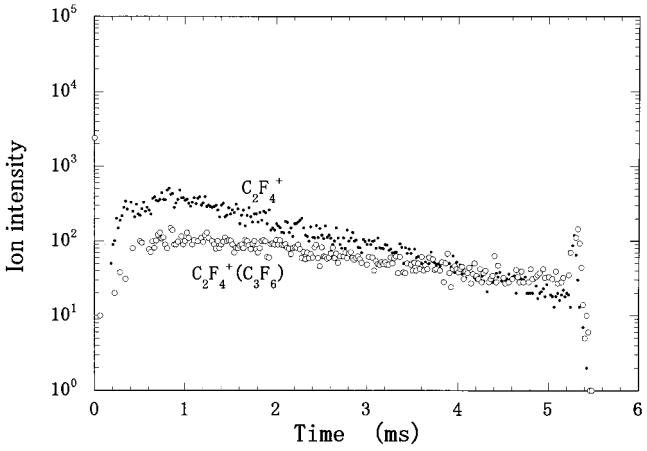


**Figure 1.** Decay profiles of $C_2F_4^+$ and $C_2F_4^+(C_3F_6)$ after the electron pulse. Ion source temperature: 190.9 K, pressure of $N_2$: 2.26 Torr, pressure of $C_3F_6$: 14.7 mTorr, integration time for $C_3F_5^+$: 30 s, integration time for $C_3F_5^+(C_3F_6)$: 120 s, 2 keV ionization electron pulse: 800 $\mu$s.

## 3. Experimental Results

**3.1. Positive-Mode Ion/Molecule Reactions in $C_3F_6$.** When 3 Torr $N_2$ major gas containing ~20 mTorr $C_3F_6$ was ionized by 2 keV electron pulse, nearly equal amounts of $C_2F_4^+$, $C_3F_5^+$, and $C_3F_6^+$ were produced as major ions. These ions did not react with $C_3F_6$ at room temperature and above. With decrease of temperature, associated ions with $C_3F_6$ were formed. However, equilibria between $C_2F_4^+$ and $C_3F_6^+$ with their associated ions were not established due to the extremely slow association reactions. In the following sections, the reactions of $C_2F_4^+$, $C_3F_5^+$, and $C_3F_6^+$ ions with $C_3F_6$ will be described.

*$C_2F_4^+$*. The associated ion $C_2F_4^+(C_3F_6)$ started to be formed when the ion source temperature was decreased below 240 K under the present experimental conditions, e.g., pressures of $N_2$ and $C_3F_6$ were ~3 Torr and ~15 mTorr, respectively. As shown in Figure 1, the equilibrium between $C_2F_4^+$ and $C_2F_4^+(C_3F_6)$ was not observed but $C_2F_4^+(C_3F_6)$ was slowly formed at the expense of $C_2F_4^+$. The slow conversion of $C_2F_4^+$ to $C_2F_4^+(C_3F_6)$ suggests either that the rate of the clustering reaction is slow due to the steric hindrance (i.e., existence of the entropy barrier in the reaction coordinate) or that the reaction of $C_2F_4^+$ with $C_3F_6$ to form $C_2F_4^+(C_3F_6)$ is irreversible and the ion $C_2F_4^+(C_3F_6)$ is not a mere cluster ion $C_2F_4^+\cdots C_3F_6$ but rather the covalently bound molecular ion $C_2F_4^+\cdot C_3F_6$. As will be described in the theoretical section, it was predicted that the positive ions $C_2F_4^+$, $C_3F_5^+$, and $C_3F_6^+$ do not form covalent bonds but rather clusters with $C_3F_6$. It was also proposed that there are three stable isomers ($n = 1$a, 1b, and 1c in Figure 9) for the cluster ions $C_2F_4^+(C_3F_6)$ and there is an entropy barrier for the formation of the most stable isomer ($n = 1$c). Thus, the slow conversion, $C_2F_4^+ \rightarrow C_2F_4^+\cdots C_3F_6$ ($n = 1$c), is likely to slow the forward rate of clustering reaction 4:

$$C_2F_4^+ + C_3F_6 + M = C_2F_4^+\cdots C_3F_6\ (n = 1c) + M\ (M{:}\text{third body}) \quad (4)$$

It was found that the clustering reaction 4 became faster with a decrease of temperature. This indicates that reaction 4 is exothermic and there is no energy barrier. At higher temperatures, the lifetime of the loosely bound intermediate complex $[C_2F_4^+\cdots C_3F_6]$* is so short that it will fall apart to the original reactants, $C_2F_4^+$ and $C_3F_6$, due to the existence of an entropy barrier to form the most stable isomer ($n = 1$c). With a decrease

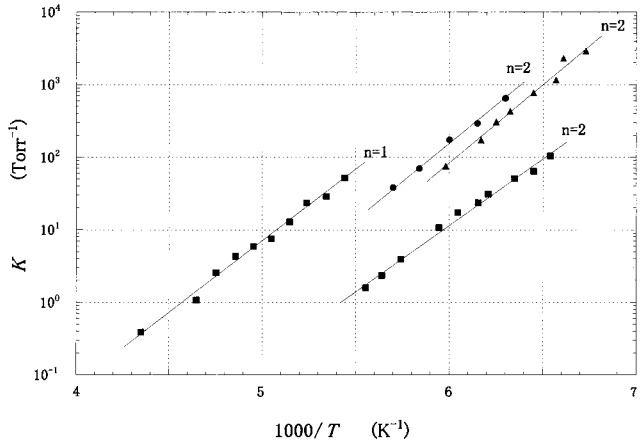


**Figure 2.** van't Hoff plots for the clustering reactions for $C_2F_4^+(C_3F_6)_1 + C_3F_6 = C_2F_4^+(C_3F_6)_2$ (●), $C_3F_5^+(C_3F_6)_{n-1} + C_3F_6 = C_3F_5^+(C_3F_6)_n$ with $n = 1$ and 2 (■), and $C_3F_6^+(C_3F_6) + C_3F_6 = C_3F_6^+(C_3F_6)_2$ (▲).

of temperature, the lifetime of the intermediate complex becomes long enough to find the bottleneck leading to the formation of the most stable cluster ion $C_2F_4^+(C_3F_6)$ ($n$ = 1c).

Below 180 K, the slow formation of the higher-order cluster ion $C_2F_4^+(C_3F_6)_2$ was observed at the expense of $C_2F_4^+(C_3F_6)$. That is, the formation of the most stable $n = 2$ cluster ion (2b in Figure 8) also experiences an entropy barrier (see the theoretical section).

$$C_2F_4^+(C_3F_6)\ (n = 1c) + C_3F_6 + M = C_2F_4^+(C_3F_6)_2\ (n = 2b) + M \quad (5)$$

Below 170 K, the intensity of $C_2F_4^+(C_3F_6)_2$ starts to increase steeply with a decrease of temperature and the equilibrium between $C_2F_4^+(C_3F_6)$ and $C_2F_4^+(C_3F_6)_2$ was established. The observed steep increase of $C_2F_4^+(C_3F_6)_2$ below 170 K is much larger than the slow growth of the same $m/z$ ion at higher temperature. The steep increase of $C_2F_4^+(C_3F_6)_2$ below ~170 K may be due to the formation of the isomeric cluster ion $C_2F_4^+(C_3F_6)(n = 1c)\cdots C_3F_6$ rather than $C_2F_4^+(C_3F_6)_2$ ($n$ = 2b) (see the theoretical section). Because the forward rate of reaction 5 is slow and the relative intensity of the isomeric cluster ion $C_2F_4^+(C_3F_6)(n = 1c)\cdots C_3F_6$ becomes much stronger than that of the $C_2F_4^+(C_3F_6)_2$ ($n$ = 2b) below 170 K, it was possible to measure the approximate equilibrium constants for the clustering reaction 6 below 170 K.

$$C_2F_4^+(C_3F_6)\ (n = 1c) + C_3F_6 + M = C_2F_4^+(C_3F_6)(n = 1c)\cdots C_3F_6 + M \quad (6)$$

The obtained van't Hoff plots were shown in Figure 2. The obtained crude thermochemical data are $-\Delta H^\circ = \sim 9.8$ kcal/mol and $-\Delta S^\circ = \sim 35$ cal/mol·K (Table 1). The large entropy change suggests that the freedom of motion in the cluster ion $C_2F_4^+(C_3F_6)(n = 1c)\cdots C_3F_6$ is highly restricted. A similar large entropy change due to the steric congestion has also been reported by Meot-Ner et al.[4] They measured the entropy change $-\Delta S^\circ$ to be 48.7 ± 2 cal/mol·K for the association reaction $t\text{-}C_4H_9^+(i\text{-}C_4H_8) + i\text{-}C_4H_8 = t\text{-}C_4H_9^+(i\text{-}C_4H_8)_2$.

*C3F5+*. Contrary to the slow clustering reactions of $C_2F_4^+$ with $C_3F_6$, the primary ion $C_3F_5^+$ was found to establish the equilibrium readily with the cluster ion $C_3F_5^+(C_3F_6)$ below 235 K. Figure 3 shows that the equilibrium between $C_3F_5^+$ and $C_3F_5^+\cdots C_3F_6$ is established even during the electron pulse. The equilibria for clustering reaction 7 could be measured with $n$ = 1 and 2.

$$C_3F_5^+(C_3F_6)_{n-1} + C_3F_6 + M = C_3F_5^+(C_3F_6)_n + M \quad (7)$$

The thermochemical data obtained from the van't Hoff plots shown in Figure 2 are listed in Table 1. The only slight decrease of the enthalpy changes ($-\Delta H^\circ_{n-1,n}$) for reaction 7, 9.2 ± 0.3 → 8.2 ± 0.3 kcal/mol for $n = 1 \rightarrow 2$ indicates that the nature of bonding in the cluster ions $C_3F_5^+(C_3F_6)_{1,2}$ is mainly electrostatic. The rather large values of the entropy changes ($-\Delta S^\circ_{0,1} = 29 \pm 3$ eu and $-\Delta S^\circ_{1,2} = 30 \pm 3$ eu) indicate that the freedom of motion in the cluster ions $C_3F_5^+(C_3F_6)_{1,2}$ is highly restricted.

*C3F6+*. The reactivity of the radical cation $C_3F_6^+$ was found to be quite similar to that of $C_2F_4^+$. This ion does not react with $C_3F_6$ above 270 K under the present experimental conditions. With decrease of temperature below 270 K, the dimer cation $C_3F_6^+(C_3F_6)$ started to be formed slowly at the expense of $C_3F_6^+$ (see Figure 4). This also suggests that there is an entropy barrier for reaction 8.

$$C_3F_6^+ + C_3F_6 + M = C_3F_6^+(C_3F_6) + M \quad (8)$$

No equilibria between $C_3F_6^+$ and $C_3F_6^+(C_3F_6)$ could be established under any experimental conditions. The growth rate of the $C_3F_6^+(C_3F_6)$ ion increased slowly with a decrease of temperature as in the case of $C_2F_4^+$. This is likely to be due to the longer lifetime of the loosely bound intermediate complex $[C_3F_6^+\cdots C_3F_6]^*$ at lower temperature resulting in the increase of the forward rate of the third-order reaction 8.

A slow growth of the trimer cation $C_3F_6^+(C_3F_6)_2$ at the expense of the dimer cation $C_3F_6^+(C_3F_6)$ was observed below 190 K as in the case of $C_2F_4^+$.

$$C_3F_6^+(C_3F_6) + C_3F_6 + M = C_3F_6^+(C_3F_6)_2 + M \quad (9)$$

The rate for the formation of the trimer cation $C_3F_6^+(C_3F_6)_2$ also increased gradually with a decrease of temperature, i.e., the overall reaction 9 has the entropy barrier but does not have the energy barrier. It was found that the intensity of the trimer cation started to grow steeply below 170 K. As in the case of $C_2F_4^+$, this is likely to be due to the formation of the less stable but entropically favored isomeric cluster ion $C_3F_6^+(C_3F_6)\cdots C_3F_6$. As shown in Figure 2, the straight van't Hoff plots were obtained in the temperature range of 170−147 K. Thermochemical data of $-\Delta H^\circ$ and $-\Delta S^\circ$ are determined to be ~8.9 kcal/mol and ~31 cal/mol·K, respectively, for reaction 10.

$$C_3F_6^+(C_3F_6) + C_3F_6 + M = C_3F_6^+(C_3F_6)\cdots C_3F_6 + M \quad (10)$$

*Proton Affinity of C3F6.* Figure 5 shows the temporal profiles of ions observed in 2.80 Torr major gas $CH_4$ and 5.2 mTorr reagent gas $C_3F_6$ at 273.4 K. The rapid decrease of $CH_5^+$ is accounted for by the steep increase of $C_3F_5^+$. We conjecture that the formation of $C_3F_5^+$ ion in Figure 5 is due to the occurrence of the proton-transfer reaction 11.

$$CH_5^+ + C_3F_6 = C_3F_5^+ + HF + CH_4 \quad (11)$$

Under any circumstances, no protonated ion $C_3F_6H^+$ could be detected. This suggests that the protonated $C_3F_6$ suffers from the prompt unimolecular dissociation to give $C_3F_5^+$ and HF. The occurrence of reaction 11 with collision rate in Figure 5 indicates that the proton affinity of $C_3F_6$ is greater than that of $CH_4$ (132.0 ± 1.5 kcal/mol[21]). On the other hand, another

**TABLE 1: Experimental ($\Delta H^o_{n-1,n}$ and $\Delta S^o_{n-1,n}$) and Calculated Thermochemical Data for the Gas-Phase Clustering Reactions for $A^-(C_3F_6)_{n-1} + C_3F_6 = A^-(C_3F_6)_n$. $\Delta H^o_{n-1,n}$ is in kcal/mol and $\Delta S^o_{n-1,n}$ is in cal/mol·K (standard state, 1 atm)[a]**

| $A^-$ | $C_2F_4^+$ | | $C_3F_5^+$ | | $C_3F_6^+$ | | $Cl^-$ | | $Br^-$ | | $I^-$ | |
|---|---|---|---|---|---|---|---|---|---|---|---|---|
| $n$ | $-\Delta H^o_{n-1,n}$ | $-\Delta S^o_{n-1,n}$ | $-\Delta H^o_{n-1,n}$ | $-\Delta S^o_{n-1,n}$ | $-\Delta H^o_{n-1,n}$ | $-\Delta S^o_{n-1,n}$ | $-\Delta H^o_{n-1,n}$ | $-\Delta S^o_{n-1,n}$ | $-\Delta H^o_{n-1,n}$ | $-\Delta S^o_{n-1,n}$ | $-\Delta H^o_{n-1,n}$ | $-\Delta S^o_{n-1,n}$ |
| 1 | | | $9.2 \pm 0.3$ | $29 \pm 3$ | | | $12.6 \pm 0.3$ | $25 \pm 3$ | $9.9 \pm 0.3$ | $19 \pm 3$ | $8.6 \pm 0.3$ | $24 \pm 3$ |
| | (16.20) | (27.3) | (7.73) | (31.5) | | | (10.0) | (22.9) | | | | |
| 2 | ~9.8 | ~35 | $8.2 \pm 0.3$ | $30 \pm 3$ | ~8.9 | ~31 | $9.6 \pm 0.3$ | $23 \pm 3$ | $8.3 \pm 0.3$ | $22 \pm 3$ | $7.7 \pm 0.3$ | $25 \pm 3$ |
| | (9.37) | | (7.84) | | | | (8.0) | | | | | |
| 3 | | | | | | | 8.9± 0.3 | $25 \pm 3$ | | | | |

[a] Values in parentheses are those obtained with B3-LYP/6-31G* electronic and zero-point vibrational energies.

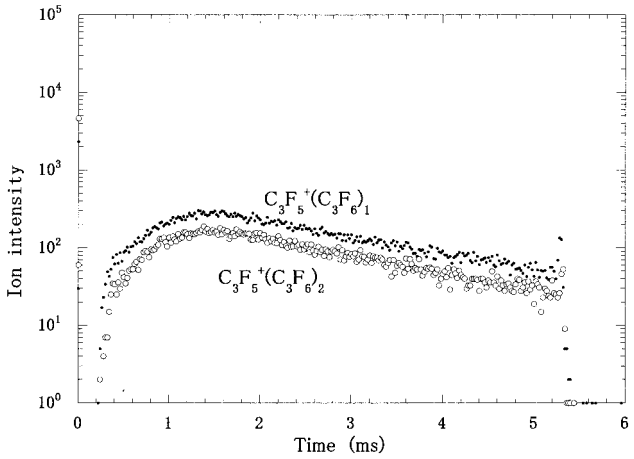


**Figure 3.** Decay profiles of $C_3F_5^+$ and $C_3F_5^+(C_3F_6)$ after the electron pulse. Ion source temperature: 212.8 K, pressure of $N_2$: 2.34 Torr, pressure of $C_3F_6$: 16.5 mTorr, integration time for $C_2F_4^+$: 240 s, integration time for $C_2F_4^+(C_3F_6)$: 240 s, 2 keV ionization electron pulse: 800 $\mu$s.

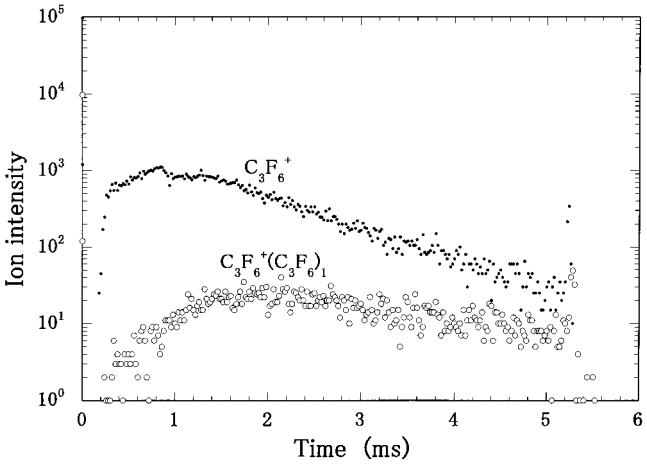


**Figure 4.** Decay profiles of $C_3F_6^+$ and $C_3F_6^+(C_3F_6)$ after the electron pulse. Ion source temperature: 227.1 K, pressure of $N_2$: 2.61 Torr, pressure of $C_3F_6$: 19.2 mTorr, integration time for $C_3F_6^+$: 240 s, integration time for $C_3F_6^+(C_3F_6)$: 120 s, 2 keV ionization electron pulse: 800 $\mu$s.

primary ion $C_2H_5^+$ generated from the major gas $CH_4$ forms the cluster ion with $C_3F_6$, $C_2H_5^+\cdots C_3F_6$, in Figure 5. Appearance of the cluster ion $C_2H_5^+\cdots C_3F_6$ and only a slow decay of $C_2H_5^+$ to form $C_3F_5^+$ suggest that the proton affinity of $C_3F_6$ is close to that of $C_2H_4$ (162.6 ± 1.5 kcal/mol[21]).

**3.2. Negative-Mode Ion/Molecule Reactions in $C_3F_6$.** *Halide Ions*. In our previous work,[9] gas-phase clustering reactions of halide ions ($X^- = F^-$, $Cl^-$, $Br^-$, and $I^-$) with $C_2H_4$ and $C_3H_6$ were studied. Bonding energies of all cluster ions were found to be less than 10 kcal/mol and no anion-initiated polymerization of $C_2H_4$ and $C_3H_6$ took place. In the present work, however,

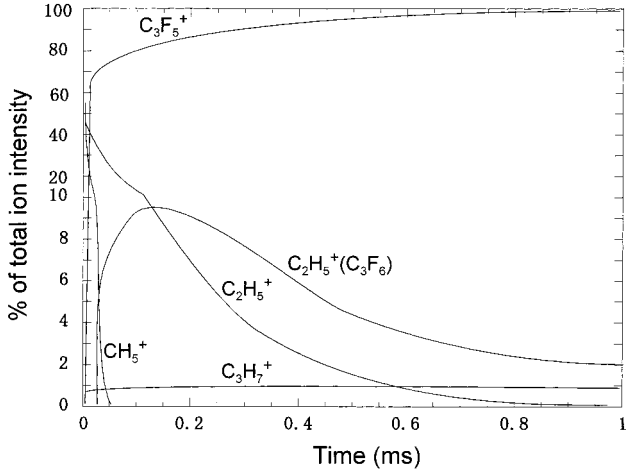


**Figure 5.** Temporal profiles of positive ions observed in 2.80 Torr major gas $CH_4$ and 5.2 mTorr reagent gas $C_3F_6$ at 273.4 K.

very rapid $F^-$-initiated polymerization reactions of $C_3F_6$ were observed (see the Theoretical Section), i.e., the occurrence of reactions 12 and 13. Here, the $F^-$ ion was generated by the dissociative electron capture by the $NF_3$ reagent gas (see the Experimental Section).

$$F^- + C_3F_6 + M \rightarrow F^-\cdot C_3F_6 + M \quad (12)$$

$$F^-\cdot C_3F_6 + C_3F_6 + M \rightarrow F^-\cdot 2C_3F_6 + M \quad (13)$$

$$F^-\cdot 2C_3F_6 + C_3F_6 + M \rightarrow F^-\cdot 2C_3F_6\cdots C_3F_6 + M \quad (14)$$

The rates of reactions 12 and 13 were found to become faster at lower temperature and the decay rates of $F^-$ and $F^-\cdot C_3F_6$ became of the order of collision rates (~$10^{-9}$ cm$^3$/molecule·s) already at 430 K and below. That is, the rates of the third-order reactions 12 and 13 are in the high-pressure limit below 430 K. Only the $F^-\cdot 2C_3F_6$ was observed after the electron pulse below 430 K under the present experimental conditions. This result is in a marked contrast to the fact that the $F^-$ ion only forms the cluster ions with $C_2H_4$ and $C_3H_6$.[9] When the ion source temperature was decreased below ~240 K, the ion $F^-\cdot 2C_3F_6$ started to react slowly with $C_3F_6$ to form the $F^-\cdot 2C_3F_6\cdots C_3F_6$ ion. No equilibrium between $F^-\cdot 2C_3F_6$ and $F^-\cdot 2C_3F_6\cdots C_3F_6$ could be observed (see Figure 6). Because reaction 14 takes place only below ~240 K and the reaction rate becomes faster at lower temperature, reaction 14 must have an entropy bottleneck. Since the $n = 3$ species $F^-\cdot 2C_3F_6\cdots C_3F_6$ was formed only below ~240 K, we conjecture that the $n = 3$ complex is not a polymerized ion but a cluster ion with the electrostatic nature.

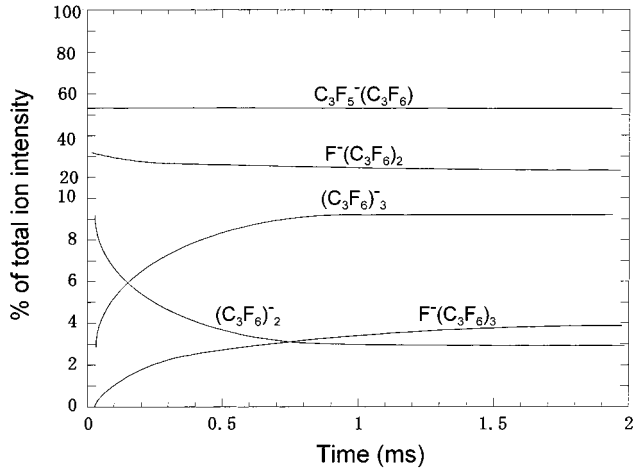


**Figure 6.** Temporal profiles of negative ions observed in 1.98 Torr major gas $N_2$, 19.6 mTorr $C_3F_6$, and 20.0 mTorr $NF_3$ at 166.0 K.

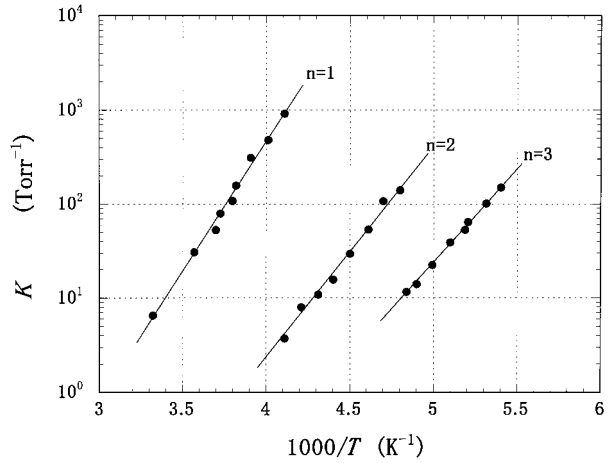


**Figure 7.** van't Hoff plots for clustering reaction, $Cl^-(C_3F_6)_{n-1} + C_3F_6 = Cl^-(C_3F_6)_n$.

It was found that other halide ions $Cl^-$, $Br^-$, and $I^-$ form the cluster ions with $C_3F_6$.

$$X^-(C_3F_6)_{n-1} + C_3F_6 + M = X^-(C_3F_6)_n + M \quad (15)$$

As an example, the van't Hoff plots for $X^- = Cl^-$ are shown in Figure 7. In the figure, there is a rather large gap between $n = 1$ and 2. This is reflected in the sudden drop in the values of $-\Delta H^o_{0,1}$ (12.6 ± 0.3 kcal/mol) → $-\Delta H^o_{1,2}$ (9.6 ± 0.3 kcal/mol) in Table 1. It seems likely that the charge transfer from $Cl^-$ to $C_3F_6$ takes place to some extent. This tendency lessens with the size of the halide ions, $Cl^- \rightarrow Br^- \rightarrow I^-$ in Table 1. In our previous work, clustering reactions $X^-(C_6F_6)_{n-1} + C_6F_6 = X^-(C_6F_6)_n$ were investigated.[22] There, $-\Delta H^o_{0,1}$ values are 15.5 (X = Cl), 13.9 (X = Br), and 11.0 (X = I) kcal/mol, respectively. Geometries of $X^-(C_6F_6)_n$ come mainly from the electrostatic interaction (the electronic net charge = −0.98 on $Cl^-$).[22] The present $X^-(C_3F_6)_n$ somewhat involves charge-transfer interactions (the net charge = −0.84 on $Cl^-$) according to the HOMO shape of $C_3F_6$. Therefore, the decrease pattern of $-\Delta H^o_{0,1}$ (12.6(X = Cl) → 9.9(X = Br) → 8.6(X = I) kcal/mol) of $X^-(C_3F_6)_1$ is slightly different from that of $X^-(C_6F_6)_1$.

*$C_3F_5^-$*. When the $C_3F_6$-containing reagent gas was ionized with 2 keV, $C_3F_5^-$ ion was formed as a major ion. This ion was converted to the $C_3F_5^-\cdot C_3F_6$ ion almost right after the electron pulse. This result is in accord with the result due to Hunter et al.[12] that the reaction product $C_3F_5^-\cdot C_3F$ is not a cluster ion but a covalently bonded molecular ion. This ion was found to be inert in all the temperature range measured (500−148 K, see Figure 6), i.e., neither the polymerization nor the clustering reaction of this ion with $C_3F_6$ took place. This may be due to the well delocalized negative charge in the polymerized ion $C_3F_5^-\cdot C_3F_6$.

*$C_3F_6^-$*. When the $C_3F_6$-containing reagent gas was ionized by a 2 keV electron beam, a small amount of the dimer anion $(C_3F_6)_2^-$ was formed right after the electron pulse, but no monomer ion $C_3F_6^-$ could be detected in all the temperature region investigated (148−500 K). These results argue for the finding of Hunter et al.[12] that the transient negative ion $C_3F_6^{-*}$ reacts with $C_3F_6$ to form the polymerized dimer anion $C_3F_6^-\cdot C_3F_6$, i.e., reactions 1−3. With decrease of temperature below 175 K, a gradual growth of the trimer anion $(C_3F_6)_3^-$ at the expense of $C_3F_6^-\cdot C_3F_6$ was observed. Figure 6 shows the temporal profiles of negative ions observed in 1.98 Torr major gas $N_2$, 19.6 mTorr $C_3F_6$, and 20.0 mTorr $NF_3$ at 166.0 K. A gradual increase of $(C_3F_6)_3^-$ suggests that the trimer anion is a weakly bound electrostatic cluster ion $C_3F_6^-\cdot C_3F_6\cdots C_3F_6$ and the clustering reaction has an entropy barrier due to the steric hindrance.

## 4. Theoretical Results and Discussion

In the previous section, reactions of positive and negative ions in $C_3F_6$ have been investigated. Electrophilic and nucleophilic centers of $C_3F_6$ are $\beta$ and α carbons, respectively, according to the extension of frontier orbitals, LUMO and HOMO. The halide ion $X^-$ is expected to attack the $\beta$ carbon

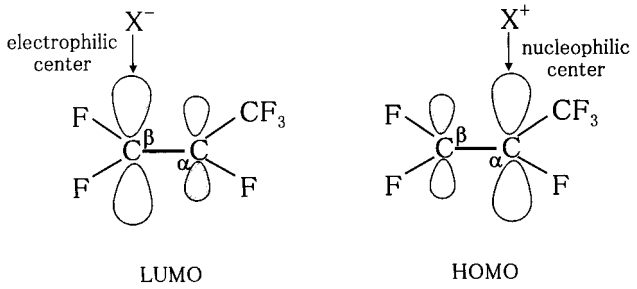


of $C_3F_6$. On the other hand, cation species ($C_2F_4^+$, $C_3F_5^+$, and proton) apparently attack the α carbon. "Apparently" means that lone-pair orbitals of fluorine substituents of the $CF_3$ group may be another electronic-charge donating sites. That is, those orbitals would block the nucleophilic center on the α carbon.

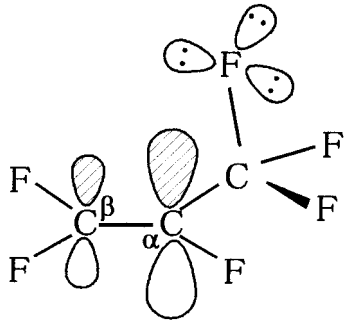

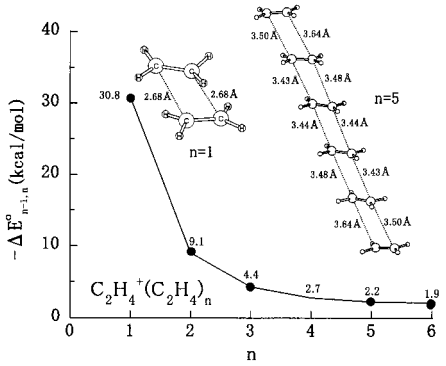


**Figure 8.** UB3LYP/6-31G* binding energies of $C_2H_4^+(C_2H_4)_{n-1} + C_2H_4 = C_2H_4^+(C_2H_4)_n$. Geometries of $n = 1$ and $n = 5$ are also shown.

**4.1. Positive-Mode Ion/Molecule Reactions in $C_3F_6$.** *$C_2F_4^+$.* $C_2F_4^+(C_3F_6)_n$ geometries are examined in comparison with those of $C_2H_4^+(C_2H_4)_n$. Figure 8 shows those of $n = 1$ and $n = 5$ of $C_2H_4^+(C_2H_4)_n$ along with the change of binding energies. The $n = 1$ structure is a compromise product of effective (HOMO→SOMO) and (HOMO→LUMO) interactions. The (HOMO→SOMO) interaction leads to a rectangle $C_2H_4^+(C_2H_4)_1$ structure, while the (HOMO→LUMO) one to a trans structure. SOMO is a singly occupied molecular orbital.

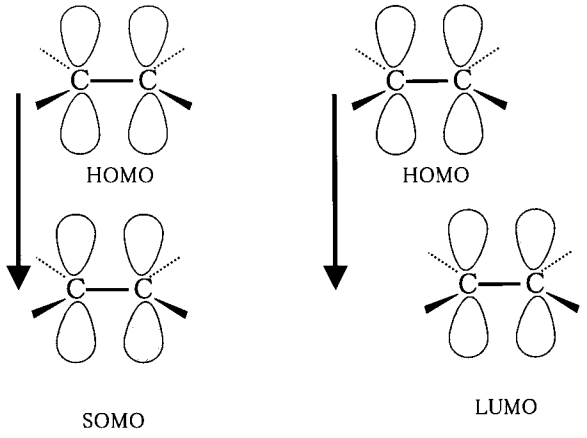


Two competitive charge-transfer interactions are directed to different geometries and cannot give new C−C covalent bonds along the axial direction. Namely, the growth of $C_2H_4^+(C_2H_4)_n$ should be terminated at the small $n$ value. The large falloff of binding energies as $n = 1 \rightarrow 2 \rightarrow 3$ and the delocalized cation character in $n = 5$ reflect the absence of the enhanced propagation function. Binding energies of 2.2 kcal/mol with $n = 5$ and 1.9 kcal/mol with $n = 6$ indicate that these $n$ values are critical for the cluster growth.[23]

Figure 9 shows geometries of $C_2F_4^+(C_3F_6)_n$. For $n = 1$, three isomers ($n = 1$a, $n = 1$b, and $n = 1$c) were obtained. No covalent bond formation is formed in these complexes. The geometries of $n = 1$a is similar to that of $C_2H_4^+(C_2H_4)_1$ and is the most unstable among three. In $n = 1$b, a fluorine lone-pair orbital participates in the charge-donation. The $n = 1$b model has a moderate stability. The $n = 1$c model is the most stable one. A lone-pair orbital is a sole electronic-charge donating

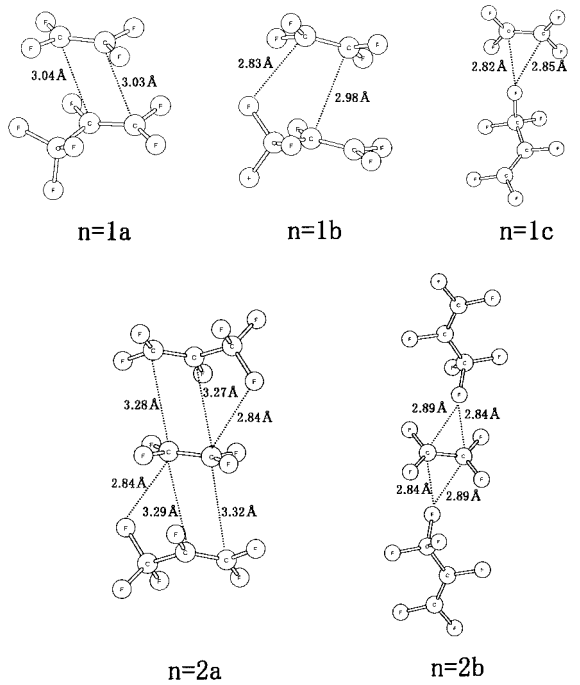


**Figure 9.** Geometries of $C_2F_4^+(C_3F_6)_n$ ($n = 1$ and 2). The $n = 1$c isomer is 3.45 and 3.26 kcal/mol more stable than $n = 1$a and $n = 1$b isomers, respectively. The $n = 2$b isomer is 1.26 kcal/mol more stable than the $n = 2$a one.

orbital toward SOMO of $C_2F_4^+$. Thus, the $C_2F_4^+(C_3F_6)_1$ geo-

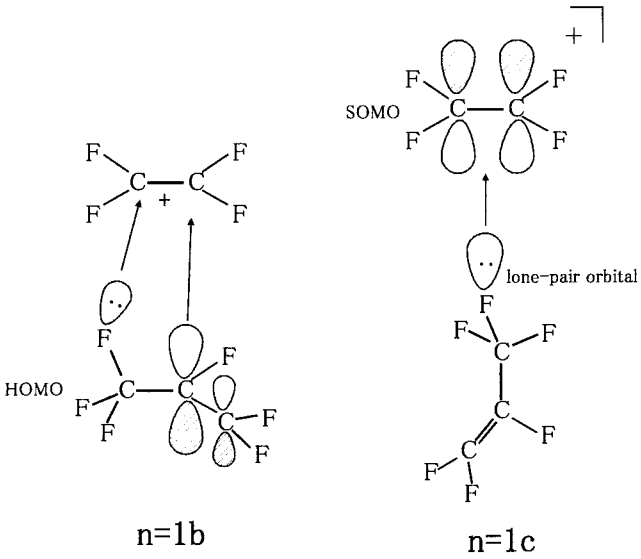


metry, $n = 1$c, is entirely different from that of $C_2H_4^+(C_2H_4)_1$ in Figure 8. Exchange repulsion between lone-pair orbitals of $C_2F_4^+$ and those of $C_3F_6$ makes models $n = 1$a and $n = 1$b less stable in Figure 9. For $n = 2$, $n = 2$b is more stable than $n = 2$a. In $n = 2$b, the cation center of $C_2F_4^+$ is sandwiched by two $C_3F_6$ ligands. Therefore, $n > 3$ clusters of $C_2H_4^+(C_3F_6)_n$ must be much less stable.

In the previous section, the cluster ions of $n = 1$ and 2 have been discussed. By analogy to the structure of $C_2H_4^+(C_2H_4)_n$ in Figure 8, those species are thought to be $n = 1$a and $n = 2$a in Figure 9. At a glance, the preceding formation of less stable $n = 1$a and $n = 2$a over that of more stable $n = 1$c and $n = 2$b seems to be curious. However, these cluster models of $n = 1$c and $n = 2$b may be generated through a "pinpoint" approach avoiding the exchange repulsion due to fluorine lone-pair

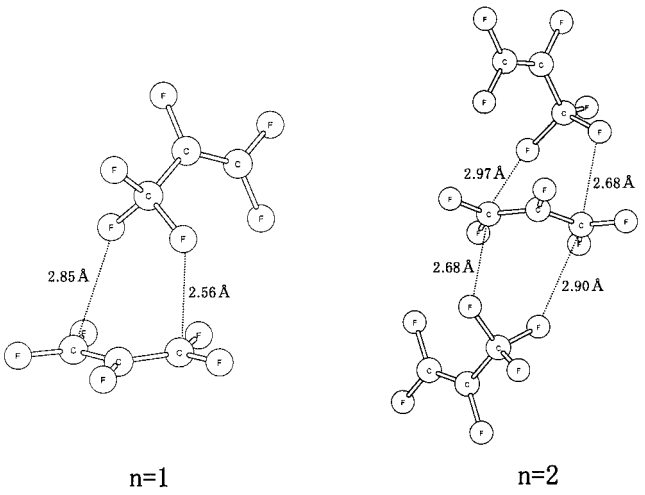


**Figure 10.** Geometries of $C_3F_5^+(C_3F_6)_n$ ($n$ = 1 and 2).

orbitals. The $CF_3$ substituent group occupies a much larger space than we think and is a source of the steric hindrance. Therefore, even if the cluster geometries of $n$ = 1c and $n$ = 2b are most stable, their formation via the primary collision is difficult. This explains the slow growth of $C_2F_4^+(C_3F_6)_n$ at the expense of $C_2F_4^+(C_3F_6)_{n-1}$. On the other hand, the isomers $n$ = 1a and $n$ = 2a are free from the contact to the bulky $CF_3$ group and would be formed primarily.

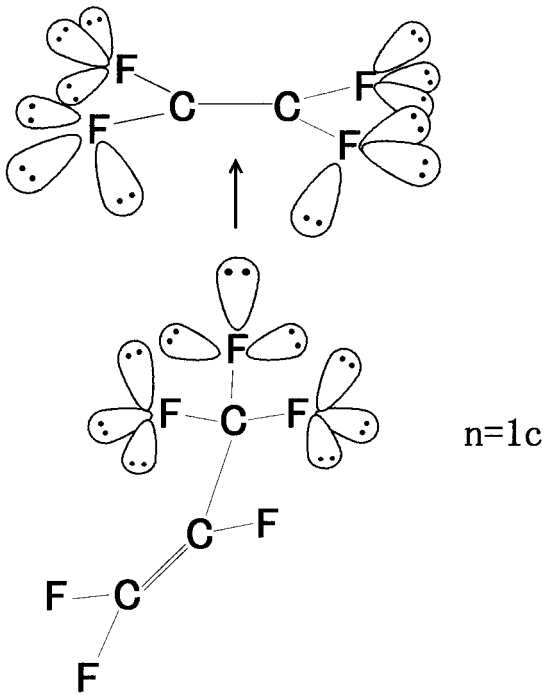


*$C_3F_5^+$*. The allyl cation-type species $C_3F_5^+$ has two equivalent terminal cation centers. Figure 10 exhibits geometries of $C_3F_5^+(C_3F_6)_1$. The two cation centers of $C_3F_5^+$ are coordinated by two fluorine substituents of the $CF_3$ group, respectively. The HOMO on the vinyl group of $C_3F_6$ cannot be the electron-donating orbital toward $C_3F_5^+$ due to the exchange repulsion. The sandwich structure of $n$ = 2 indicates that $n$ > 3 clusters are improbable for $C_3F_5^+(C_3F_6)_n$. The cation centers in $C_3F_5^+$ are two terminal carbon atoms, and the cluster formation is easier than that of $C_2F_4^+(C_3F_6)_n$ owing to the smaller steric congestion. The ready formation is consistent with the quick establishment of the equilibria for reaction 7.

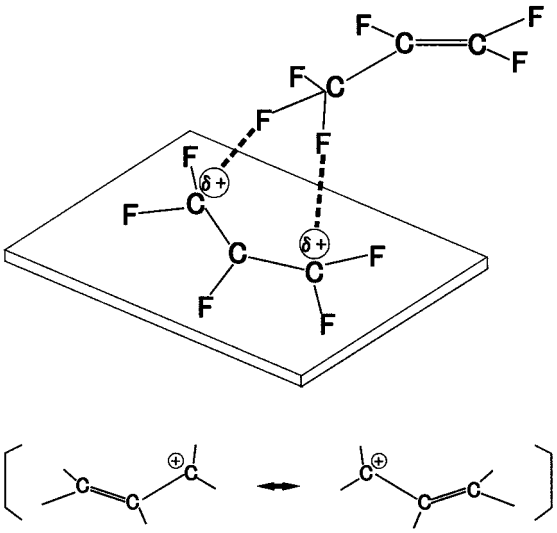

*Proton Affinity of $C_3F_6$.* As discussed in the Experimental Results section, proton transfer to $C_3F_6$ does not form the stable protonated parent ion but rather appears to decompose immediately into $C_3F_5^+$ + HF (reaction 11. When the proton attacks HOMO of $C_3F_6$, $H^+(C_3F_6)$ would be generated. In fact, two geometric isomers of the protonated $C_3F_6$ have been obtained and are shown in Figure 11. Proton affinities calculated by two ways, B3-LYP/6-31G* and G2MP2, are also shown in the Figure. Noteworthy are similar values of two isomers. Since G2MP2 values are more reliable than B3LYP/6-31G*,[19] the F protonated species is slightly more stable than C protonated one. But, the energy difference is too small to describe the exclusive formation of not $H^+C_3F_6$ but ($C_3F_5^+$ + HF). The HOMO extension is blocked by lone-pair orbitals, and the proton migrated from $CH_5^+$ is trapped by a lone-pair electron regardless of the intrinsic basicity of the α carbon at HOMO. The proton affinity of $C_3F_6$ is 157.3 kcal/mol according to the G2MP2 enthalpy.

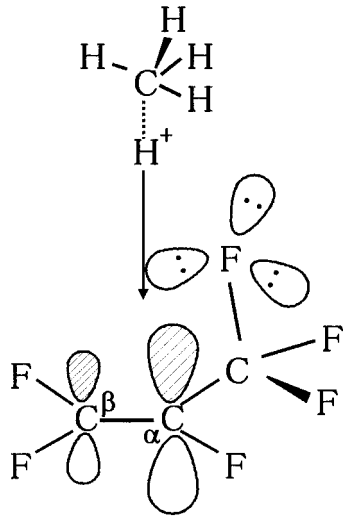

*Halide Ions.* As stated in the beginning of this section, LUMO is extended largely on the $\beta$ carbon. According to the FMO prediction, geometries of $X^-(C_3F_6)_n$ (X = F and Cl with $n$ = 1 and 2) were examined and are shown in Figure 12. $F^-(C_3F_6)_1$ is found to be of $C_s$ symmetry and the original fluoride ion is a fluorine substituent in $F^-(C_3F_6)_1$. A similar $F^-$ quench to neutral fluorinated ligands was reported in $F^- + C_6F_6 \rightarrow C_6F_7^-$ (Meisenheimer complex).[24] In $F^-(C_3F_6)_1$, the central carbon

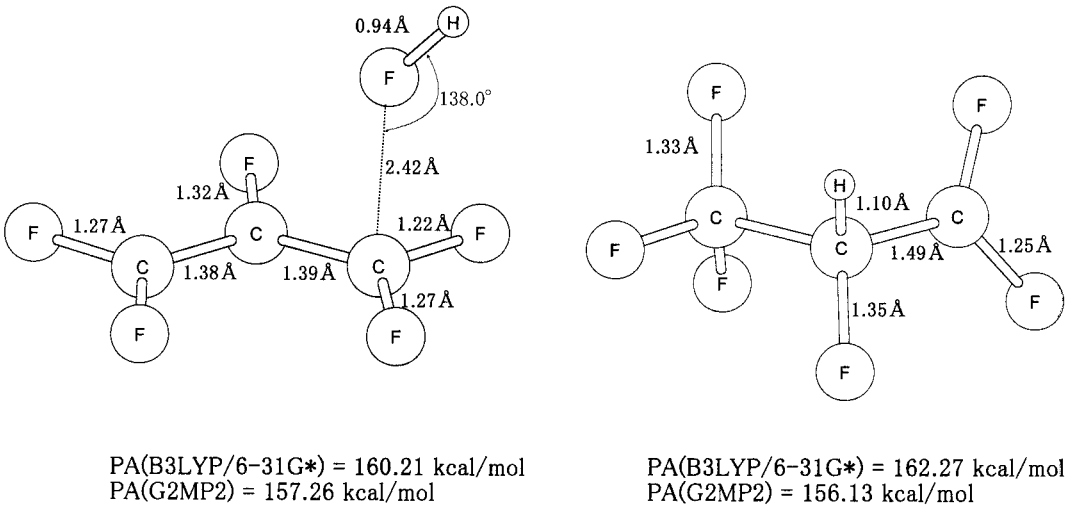


PA(B3LYP/6-31G*) = 160.21 kcal/mol
PA(G2MP2) = 157.26 kcal/mol

PA(B3LYP/6-31G*) = 162.27 kcal/mol
PA(G2MP2) = 156.13 kcal/mol

**Figure 11.** Geometric isomers of the protonated $C_3F_6$. The computed proton affinities are also shown in kcal/mol.

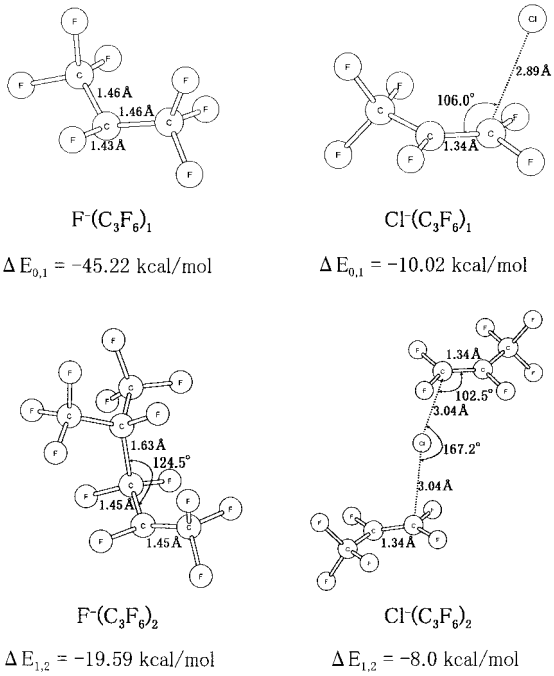


$F^-(C_3F_6)_1$ $\Delta E_{0,1}$ = −45.22 kcal/mol

$Cl^-(C_3F_6)_1$ $\Delta E_{0,1}$ = −10.02 kcal/mol

$F^-(C_3F_6)_2$ $\Delta E_{1,2}$ = −19.59 kcal/mol

$Cl^-(C_3F_6)_2$ $\Delta E_{1,2}$ = −8.0 kcal/mol

**Figure 12.** Geometries of $X^-(C_3F_6)_n$ ($n$ = 1 and 2) clusters.

atom is so nucleophilic that an axial C−C bond (1.633 Å) is formed in $F^-(C_3F_6)_2$ and the anion center is effectively transmitted to the second central carbon. A polymerization in reactions 12 and 13 is likely. In contrast, the $Cl^-(C_3F_6)_n$ cluster is found to be of normal long-range interaction in Figure 12.

In Table 1, B3LYP/6-31G* (cation clusters) and B3LYP/6-31+G* (halide-ion clusters) binding energies and entropy changes are shown in parentheses. Although those energies are somewhat underestimated relative to those measured here, they seem to be in fair agreement.

## 5. Concluding Remarks

The positive- and negative-mode ion/molecule reactions in $C_3F_6$ were investigated. In the positive-ion mode, the forward rates of the clustering reactions of radical cations $C_2F_4^+$ and $C_3F_6^+$ with $C_3F_6$ were found to be extremely slow. This is due to the steric hindrance (i.e., entropy barrier) for the formation of the most stable isomers. With decrease in temperature, the formation of less stable but entropically more favored isomeric cluster ions becomes prevalent. The equilibria for the clustering reactions of the closed-shell $C_3F_5^+$ ion with $C_3F_6$ were established even during the electron pulse. This is due to the absence of the steric crowd for the formation of cluster ions $C_3H_5^+$-$(C_3F_6)_{1,2}$. The proton affinity of $C_3F_6$ was found to be smaller but close to that for ethylene (162.6 ± 1.5 kcal/mol[21]). The G2MP2 calculated value is 157.26 kcal/mol. In cation ($X^+$) clusters, the nucleophilic center of HOMO (i.e., α carbon of $C_3F_6$) is blocked by lone-pair orbitals of the $CF_3$ group, which leads to the $X^+\cdots F_3C-CF=CF_2$ coordination. In the negative-ion mode, both closed shell ions $F^-$ and $C_3F_5^-$ and an open-shell ion $C_3F_6^-$ were found to react with $C_3F_6$ to form the polymerized ions. The high reactivity of $C_3F_6$ in the negative-mode ion/molecule reactions is in a marked contrast to the less reactive $C_3H_6$.[9] Observed higher reactivity of $C_3F_6$ is due to the perfluoro effect, i.e., the energy levels of LUMO ($\pi^*$) is lowered by the F-atom substitution and the charge transfer from the negative ions to the $\beta$ carbon of the $\pi^*$ orbital (LUMO) of $C_3F_6$ is favored. The observed trend of $C_3F_6$ for the formation of the negative-mode polymerized products may be useful for the semiconductor fabrication as an etchant because the side wall etching may be suppressed by the formation of polymer film on the surface of the side wall.

## References and Notes

(1) Lias, S. G.; Ausloos, P. In *Ion−Molecule Reactions, Their Role in Radiation Chemistry*; American Chemical Society, Washington, DC, 1975.
(2) Kebarle, P.; Haynes, R. M. *J. Chem. Phys.* **1967**, *47*, 1676.
(3) Tzeng, W.-B.; Ono, Y.; Linn, S. H.; Ng, C. Y. *J. Chem. Phys.* **1985**, *83*, 2803.
(4) Meot-Ner, M.; Sieck, L. W.; El-Shall, M. S.; Daly, G. M. *J. Am. Chem. Soc.* **1995**, *117*, 7737.
(5) El-Shall, M. S.; Daly, G.M.; Yu, Z.; Meot-Ner, M. *J. Am. Chem. Soc.* **1995**, *117*, 7744.
(6) Lytkey, M. Y. M.; Rycroft, T.; Garvey, J. F. *J. Phys. Chem.* **1996**, *100*, 6427.
(7) Zhong, O.; Poth, L.; Shi, Z,; Ford, J. V.; Castleman, A. W., Jr. *J. Phys. Chem.* **1997**, *101*, 4203.
(8) Hiraoka, K.; Kojima, T.; Sugiyama, T.; Katsuragawa, J. *J. Mass Spectrom. Soc. Jpn.* **1999**, *47*, 67.
(9) Hiraoka, K.; Katsuragawa, J.; Sugiyama, T.; Kojima, T.; Yamabe, S. *J. Am. Soc. Mass Spectrom.* **2001**, *12*, 144.
(10) Brundle, C. R.; Robin, M. B.; Kuebler, N. A.; Basch, H. *J. Am. Chem. Soc.* **1972**, *94*, 1451.
(11) Morris, R. A.; Viggiano, A. A.; Paulson, J. F. *J. Phys. Chem.* **1993**, *97*, 6208.
(12) Hunter, S. R.; Christophorou, L. G.; McCorkle, D. L.; Sauers, I.; Ellis, H. W.; James, D. R. *J. Phys. D: Appl. Phys.* **1983**, *16*, 573.
(13) Jarvis, G. K.; Peverall, R.; Mayhew, C. A. *J. Phys. B: At. Mol. Opt. Phys.* **1996**, *29*, L713.
(14) Kebarle, P. In *Techniques for the Study of Ion−Molecule Reactions*; Farrar, J.M., Saunders, W.H., Jr., Eds.; Wiley: New York, 1971; p 221.

(15) Hiraoka, K.; Yamabe, S. In *Dynamics of Excited Molecules*; Kuchitsu, K. Ed.; Elsevier: Amsterdam, 1994, p 399.
(16) Becke, A. D. *J. Chem. Phys.* **1993**, *98*, 5648.
(17) Clark, T.; Chandrasekhar, J.; Spitznagel, G. W.; Schleyer, P. v. R. *J. Compt. Chem.* **1983**, *4*, 294.
(18) Curtiss, L. A.; Raghavachari, K.; Pople, A. *J. Chem. Phys*. **1993**, *98*, 1293.
(19) Foresman, J. B.; Frisch, *Æ. Exploring Chemistry with Electronic Structure Methods*, 2nd ed.; Gaussian, Inc.: Pittsburgh, PA, 1995; Chapter 7, p 158.
(20) Frisch, M. L.; Trucks, G. W.; Schlegel, H. B.; Scuseria, G. E.; Robb, M. A.; Cheesemen, J. R.; Zakrzewski, V. G.; Montgomery, J. A., Jr.; Stratmann, R. E.; Burant, J. C.; Dapprich, S.; Millam, J. M.; Daniels, A. D.; Kudin, K. N.; Strain, M. C.; Farkas, O.; Tomasi, J.; Barone, V.; Cossi, M.; Cammi, R.; Mennucci, B.; Pomelli, C.; Adamo, C.; Clifford, S.; Ochterski, J.; Petersson, G. A.; Ayala, P. Y.; Cui, Q.; Morokuma, K.; Malick, D. K.; Rabuck, A. D.; Raghavachari, K.; Foresman, J. B.; Cioslowski, J.; Ortiz, J.V.; Baboul, A. G.; Stefanov, B. B.; Liu, G.; Liashenko, A.; Piskorz, P.; Komaromi, I.; Gomperts, R.; Martin, R. L.; Fox, J.; Keith, T.; Al-Laham, M. A.; Peng, C. Y.; Nanayakkara, A.; Gonzalez, C.; Challacombe, M.; Gill, P. M. W.; Johnson, B.; Chen, W.; Wong, M. W.; Andres, J. L.; Gonzalez, J. C.; Head-Gordon, M.; Replogle, E. S.; Pople, J. A. *Gaussian 98*, *Revision A.7*; Gaussian, Inc.: Pittsburgh, PA, 1998.
(21) Lias, S. G.; Liebman, J. F.; Levin, R. D. *J. Phys. Chem. Ref. Data* **1984**, *13*, 695.
(22) Hiraoka, K.; Mizuse, S.; Yamabe, S. *J. Phys. Chem*. **1987**, *91*, 5294.
(23) Besides formation of $C_2H_4^+(C_2H_4)_n$ clusters in Figure 8, that of cycloalkane radical cations (polymerization) is conceivable. The cyclobutane radical cation $C_4F_8^+$ ($n = 1$) involves the largest ring strain, i.e., instability but is 3.3 kcal/mol more stable than the cluster-type isomer. Therefore, with the excess energy supply, cyclobutane radical cations and their fragments would be yielded. On the other hand, the present experiments are not concerned with C−C covalent bond formation.
(24) Hiraoka, K.; Mizuse, S.; Yamabe, S. *J. Chem. Phys*. **1987**, *87*, 3647.